JNS

CLINICAL ARTICLE

J Neurosurg 141:291–305, 2024

Eloquent noneloquence: redefinition of cortical eloquence based on outcomes of superficial cerebral cavernous malformation resection

Benjamin K. Hendricks, MD,[1] Lea Scherschinski, MD,[1] Jubran H. Jubran, MD,[2] Nicholas B. Dadario, BS,[3] Katherine Karahalios, MS,[1] Dimitri Benner, BS,[1] Danielle VanBrabant, MSMI, CMI,[1] and Michael T. Lawton, MD[1]

[1]Department of Neurosurgery, Barrow Neurological Institute, St. Joseph's Hospital and Medical Center, Phoenix, Arizona; [2]University of Arizona College of Medicine–Phoenix, Arizona; and [3]Robert Wood Johnson Medical School, Rutgers University, New Brunswick, New Jersey

OBJECTIVE Cerebral cavernous malformations (CMs) are pathological lesions that cause discrete cortical disruption with hemorrhage, and their transcortical resections can cause additional iatrogenic disruption. The analysis of microsurgically treated CMs might identify areas of "eloquent noneloquence," or cortex that is associated with unexpected deficits when injured or transgressed.

METHODS Patients from a consecutive microsurgical series of superficial cerebral CMs who presented to the authors' center over a 13-year period were retrospectively analyzed. Neurological outcomes were measured using the modified Rankin Scale (mRS), and new, permanent neurological or cognitive symptoms not detected by changes in mRS scores were measured as additional functional decline. Patients with multiple lesions and surgical encounters for different lesions within the study interval were represented within the cohort as multiple patient entries. Virtual object models for CMs and approach trajectories to subcortical lesions were merged into a template brain model for subtyping and Quicktome connectomic analyses. Parcellation outputs from the models were analyzed for regional cerebral clustering.

RESULTS Overall, 362 CMs were resected in 346 patients, and convexity subtypes were the most common (132/362, 36.5%). Relative to the preoperative mRS score, 327 of 362 cases (90.3%) were in patients who improved or remained stable, 35 (9.7%) were in patients whose conditions worsened, and 47 (13.0%) were in patients who had additional functional decline. Machine learning analyses of lesion objects and trajectory cylinder mapping identified 7 hotspots of novel eloquence: supplementary motor area (bilateral), anterior cingulate cortex (bilateral), posterior cingulate cortex (bilateral), anterior insula (left), frontal pole (right), mesial temporal lobe (left), and occipital cortex (right).

CONCLUSIONS Transgyral and transsulcal resections that circumvent areas of traditional eloquence and navigate areas of presumed noneloquence may nonetheless result in unfavorable outcomes, demonstrating that brain long considered by neurosurgeons to be noneloquent may be eloquent. Eloquent hotspots within multiple large-scale networks redefine the neurosurgical concept of eloquence and call for more refined dissection techniques that maximize transsulcal dissection, intracapsular resection, and tissue preservation. Human connectomics, awareness of brain networks, and prioritization of cognitive outcomes require that we update our concept of cortical eloquence and incorporate this information into our surgical strategies.

https://thejns.org/doi/abs/10.3171/2023.12.JNS232588

KEYWORDS cavernous malformation; connectome; eloquence; large-scale brain network; machine learning; noneloquence; transgyral approach; transsulcal approach; vascular disorders

ABBREVIATIONS AUC = area under the curve; AVM = arteriovenous malformation; CEN = central executive network; CM = cavernous malformation; DAN = dorsal attention network; DMN = default mode network; EEG = electroencephalography; fMRI = functional MRI; HCP = Human Connectome Project; LN = limbic/paralimbic network; mRS = modified Rankin Scale; SEZ = safe entry zone; SMA = supplementary motor area; SMN = sensorimotor network; SN = salience network; SVC = support vector classification; VAN = ventral attention network; VN = visual network.

SUBMITTED November 10, 2023. **ACCEPTED** December 12, 2023.
INCLUDE WHEN CITING Published online March 8, 2024; DOI: 10.3171/2023.12.JNS232588.

The often-quoted statement that "humans use only 10% of their brains," a false attribution to Albert Einstein or a misinterpretation of William James' work, suggests that parts of the brain with distinct and important functions, like the primary motor, sensory, and visual cortices, are islands in a sea of unused brain.[1] As inaccurate as this so-called "10% myth" may seem to neurosurgeons, our concept of brain eloquence is strikingly similar. When Spetzler and Martin incorporated the eloquence of the brain adjacent to an arteriovenous malformation (AVM) as 1 of 3 variables in their grading system for predicting the risk of microsurgical arteriovenous malformation resection, only the sensorimotor, visual, and language cortices were included in their definition of eloquent cortex.[2] Implicit in this definition was that other cortical areas are noneloquent and can be transgressed with impunity.

The Human Connectome Project (HCP) transformed our understanding of brain circuitry by mapping short- and long-range bundles of nerve fibers interconnecting regions of the brain structurally and functionally in more than 1000 human participants using sophisticated imaging technologies like high-resolution MRI, resting-state and task-based functional MRI (fMRI), diffusion MRI, magnetoencephalography, and electroencephalography (EEG).[3–7] The HCP and connectomics led to the discovery of large-scale brain networks, which are widespread, seemingly unrelated brain regions or parcels anatomically wired together with synchronized activity. Many large-scale brain networks have been identified: 1) the default mode network (DMN), 2) the salience network (SN), 3) the dorsal attention network (DAN), 4) the central executive network (CEN), 5) the sensorimotor network (SMN), 6) the visual network (VN), and 7) the limbic/paralimbic network (LN).[8–11] Cognition can be understood not as individual parcels working in isolation but as multiple parcels in a network firing together and multiple networks working with orchestrated interactivity. Higher cognitive function may be the result of tightly coordinated electrical signaling between networks. Conversely, neuropsychiatric disorders such as depression, anxiety, autism, and schizophrenia may be the result of dyscoordination and disruption of signaling between networks.

Surveying the map of large-scale brain networks suggests that every cortical parcel is part of a network, and the entire cerebrum is involved in cognitive function.[9,11] This finding is at odds with our neurosurgical concept of eloquence and raises questions: is any cortex noneloquent, and for neurosurgeons, are areas long considered noneloquent truly eloquent? The answers have a profound impact on surgical strategy, and consequently, technology has emerged to integrate brain networks into preoperative planning and intraoperative navigation. Quicktome (Omniscient Neurotechnology) is an example that uses resting-state MRI to build patient-specific brain maps, including network templates, constrained spherical deconvolution-based tractography, and structural connectivity atlases. Informed neurosurgical decision-making that preserves brain networks during transcortical procedures is a step toward modernizing our concept of eloquence and incorporating it into contemporary neurosurgical practice.

Cerebral cavernous malformations (CMs) are pathological lesions that cause discrete cortical disruption with hemorrhage, and their transcortical resections can cause additional iatrogenic disruption. Therefore, a collection of microsurgically treated CMs provides a unique opportunity to study areas of "eloquent noneloquence." Neurosurgeons plan their resections to avoid transgressing eloquent brain tissue, instead selecting alternative routes through noneloquent tissue that reaches the target. An assessment of neurological and cognitive morbidity in these patients could identify areas thought to be cortical safe entry zones (SEZs) that are not safe but eloquent. Like established SEZs for brainstem CMs, cortical SEZs must be areas of true noneloquence that can be transgressed to access the pathology. We hypothesize that cortical SEZs can be established for cerebral CMs as the areas around and away from eloquent noneloquence. In this study, we analyzed the results from a large patient series of superficial cerebral CMs resected microsurgically using a combination of traditional neurological outcome measures, additional measures to detect functional decline, Quicktome algorithms, and sophisticated machine learning techniques. We proposed that the neurosurgical concept of eloquence could be redefined by mapping hotspots or cortical areas of eloquence in areas formerly considered to be noneloquent. We also proposed that minimizing transgression through these hotspots of eloquent noneloquence would improve our microsurgical techniques and patient outcomes.

Methods

Patients

The patients in this study were retrospectively analyzed from a consecutive series of adult patients undergoing surgery for superficial cerebral CMs at our center from November 2008 through June 2021 by two neurosurgeons (M.T.L. and Robert F. Spetzler). Anatomically, only lesions within the superficial cerebral parenchyma that did not involve the thalamus, basal ganglia, or brainstem were included. Cortical CMs were defined as any lesion in the cerebrum where the closest presentation was ≤ 1 cm from the cortical surface. Subcortical CMs were defined as any lesion in the cerebrum where the closest presentation was > 1 cm deeper than the cortical surface. In other words, subcortical CMs required significant transgression into the cerebral cortex, whereas cortical CMs did not.

Outcomes

Neurological outcomes were measured by a dedicated clinical research nurse using the modified Rankin Scale (mRS). Good outcomes were defined as mRS scores ≤ 2, and poor outcomes were defined as mRS scores > 2. Relative outcomes were measured as the difference between mRS scores at the preoperative baseline and at the last available postoperative examination. Good outcomes were defined as unchanged or improved mRS scores, and poor outcomes as worsened mRS scores. Patients with multiple lesions and surgical encounters for different lesions within the study interval were represented within the cohort as multiple patient entries, bringing the total number of cases to 362 (equivalent to the number of lesions). Patients were

excluded if neither a discharge mRS score nor follow-up evaluation was obtained, or adequate pre- and postoperative T1-weighted MR images were unavailable.

Additional functional decline was defined as new, permanent neurological symptoms present postoperatively or at clinical follow-up that were attributable to CM resection and not detected by changes in mRS scores. Symptoms indicating functional decline included new sensory, motor, cranial nerve, and speech deficits. Cognitive deficits held particular interest and included learning, memory, motor planning, attention, and social dysfunction deficits. They were identified in outpatient clinic records by any of the following: 1) the need for rehabilitation or physical therapy beyond 6 weeks postoperatively, 2) additional MRI after the routine 6-month surveillance, 3) additional office visits after the routine 6-month follow-up, and 4) referrals to neuropsychologists or psychiatrists. New-onset seizures or increases in seizure frequency were excluded as additional functional decline.

MRI Protocols

MRI was performed for all patients preoperatively to generate T1-weighted volumetric models of the CMs for intraoperative neuronavigation and postoperatively to confirm complete resection and to generate volumetric models of the surgical corridor. In addition, diffusion tractography images were acquired with the following parameters: Siemens Skyra 3.0T MRI scanner, with 10 b = 0 baseline images and a b = 1000 shell with 64-direction acquisition, field of view 224 mm × 224 mm, slice thickness 2 mm, 0-mm gap between slices with no overlap, full brain coverage, isotropic voxels, and square 112 × 112 matrix.

Network templates were created using Quicktome. Diffusion tractography generated with a constrained spherical deconvolution algorithm[12] was used to construct a template brain–specific version of the HCP-MMP1 (multimodal parcellation version 1)[13] atlas with machine learning.[14] The Quicktome program maps 379 parcels, including 180 cortical regions per hemisphere and 19 subcortical structures, such as the caudate nuclei, putamen, globus pallidus, amygdala, thalamus, ventral diencephalon, and nucleus accumbens. Large-scale brain networks, which are sets of cortical parcels and the white matter tracts connecting them, were defined on this template atlas leveraging insights from fMRI, blood oxygen level–dependent signals, and published meta-analyses.[15–21] Large-scale brain networks that synchronize their activity to serve a common function were identified using Quicktome and were mapped within the template model.

Assessment of Surgical Approaches

The effects of the surgical approach on each patient were assessed with preoperative and postoperative MRI and patient outcome (mRS score) measures. The CM and any associated hemorrhage were manually traced by a trained neurosurgeon on the template brain based on an overlay of T1-weighted images of the patient's CM. The surgical approach to cortical CMs was estimated using the lesion object or CM volume. In contrast, the surgical approach to subcortical CMs was estimated using the lesion object plus a cylinder object 2 cm in diameter from the cortical entry site to the CM (trajectory). These virtual space objects were transformed into NIFTI (neuroimaging informatics technology initiative) format and anatomically aligned with the template brain on the basis of the anterior commissure–posterior commissure and lateral convexity. This combined object was then warped into MNI-152 space (Montreal Neurological Institute's 152-brain template), and the HCP-MMP atlas was warped to the template brain using the Quicktome algorithm.

All parcels belonging to large-scale brain networks that collided with the lesion object or trajectory cylinder were identified, and collisions were quantified by the number of voxels. The degree of collision or transgression of a network was modeled using machine learning algorithms with varied thresholds from 1 to 10,000 voxels. A threshold of 200 voxels optimized model performance for lesion object transgression analysis. A threshold of 500 voxels optimized model performance for trajectory transgression analysis, given that the cylindrical object method tended to overestimate tissue transgression of the cortical folds for the transsylvian, transsulcal, and interhemispheric approaches.

Statistical Analysis

A non–black box machine learning approach designed for categorical data was used to determine which parcels and large-scale brain networks were affected in patients who experienced poor outcomes or additional functional decline. Logistic regression, support vector classification (SVC), and the categorical Naive Bayes algorithm facilitated the extraction of feature weights after training the model. The class imbalance was addressed using the synthetic minority oversampling technique, and models were evaluated for maximal area under the curve (AUC) and accuracy. These models were adopted for the 2 transgression analyses: lesional object mapping and transcortical trajectory mapping. The general list of features with feature weights > 0.2 was similar for both modeling techniques when the models exhibited an AUC > 0.7, suggesting robust modeling approaches. SVC with a linear kernel (chosen to permit demonstration of feature importance) outperformed the other models. All modeling was performed with Python (version 3, Python Software Foundation) using the Scikit-learn package.

Results

Patient Characteristics

Of the 434 superficial cerebral CMs that were microsurgically resected during the 13-year study period, 72 were excluded due to inadequate imaging or follow-up data, leaving a study cohort of 362 CMs in 346 patients. The mean (SD) patient age at surgery was 39.3 (15.74) years; 59% of patients were women (204/346), and 41% were men (142/346). Because patients with multiple lesions and surgical encounters for different lesions were represented in the patient cohort with multiple entries in the analyses, the number of cases was equal to the number of CMs. Convexity CMs were the most common su-

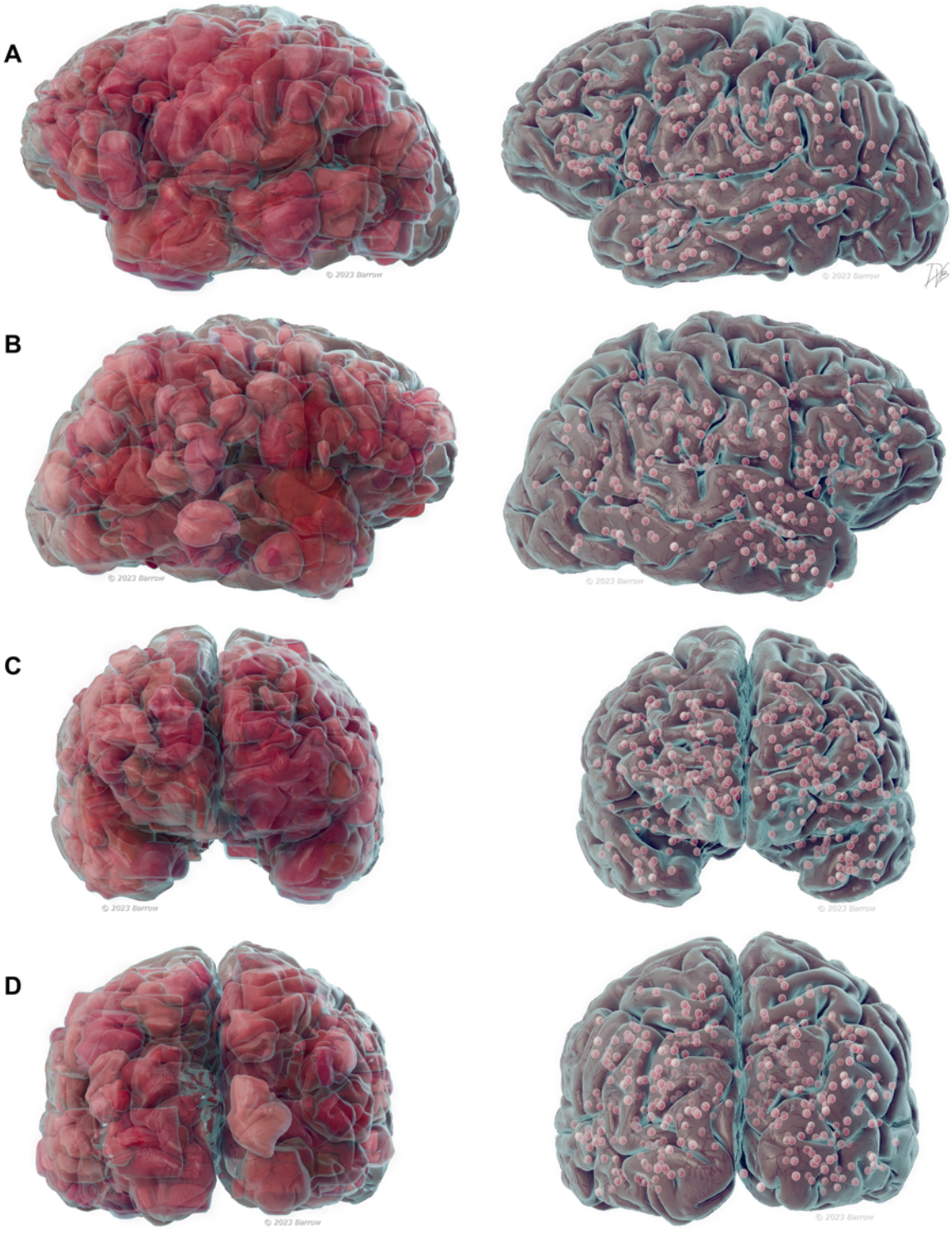

FIG. 1. Left (**A**) and right (**B**) lateral views and anterior (**C**) and posterior (**D**) views showing individual virtual cerebral CMs (*left*) mapped to the template cerebral model (*right*). Used with permission from Barrow Neurological Institute, Phoenix, Arizona.

perficial cerebral subtype (132/362, 36.5%), followed by medial (78, 21.5%), basal (72, 19.9%), and sylvian (80, 22.1%) subtypes (Fig. 1). The most common lobar locations were frontal (155/362, 42.8%), parietal (89, 24.6%), and temporal (87, 24.0%). Most CMs (302/362, 83.4%) were cortical, and 60 (16.6%) were subcortical. The mean (SD) lesion volume was 4.68 (9.034) cm^3. Of the 379 parcels identified in Quicktome, 359 were occupied by a le-

TABLE 1. Cerebral CM subtypes by patient outcome status

Subtype	Total CMs (n = 362)	No. of CMs by Patient Outcome				
		Improved/Unchanged	Worsened	Additional Decline	Unfavorable	Favorable
Frontal	155/362 (42.8)	140/327 (42.8)	15/35 (42.9)	18/47 (38.3)	33/82 (40.2)	122/280 (43.6)
Medial	42/155 (27.1)	38/140 (27.1)	4/15 (26.7)	6/18 (33.3)	10/33 (30.3)	32/122 (26.2)
Convexity	56/155 (36.1)	52/140 (37.1)	4/15 (26.7)	7/18 (38.9)	11/33 (33.3)	45/122 (36.9)
Basal	34/155 (21.9)	29/140 (20.7)	5/15 (33.3)	2/18 (11.1)	7/33 (21.2)	27/122 (22.1)
Sylvian	23/155 (14.8)	21/140 (15.0)	2/15 (13.3)	3/18 (16.7)	5/33 (15.2)	18/122 (14.8)
Parietal	89/362 (24.6)	76/327 (23.2)	13/35 (37.1)	10/47 (21.3)	23/82 (28.0)	66/280 (23.6)
Medial	24/89 (27.0)	22/76 (28.9)	2/13 (15.4)	2/10 (20.0)	4/23 (17.4)	20/66 (30.3)
Convexity	32/89 (36.0)	27/76 (35.5)	5/13 (38.5)	5/10 (50.0)	10/23 (43.5)	22/66 (33.3)
Sylvian	33/89 (37.1)	27/76 (35.5)	6/13 (46.2)	3/10 (30.0)	9/23 (39.1)	24/66 (36.4)
Occipital	31/362 (8.6)	29/327 (8.9)	2/35 (5.7)	2/47 (4.3)	4/82 (4.9)	27/280 (9.6)
Medial	5/31 (16.1)	5/29 (17.2)	0/2 (0)	0/2 (0)	0/4 (0)	5/27 (18.5)
Convexity	14/31 (45.2)	13/29 (44.8)	1/2 (50)	1/2 (50.0)	2/4 (50)	12/27 (44.4)
Basal	12/31 (38.7)	11/29 (37.9)	1/2 (50)	1/2 (50.0)	2/4 (50)	10/27 (37.0)
Temporal	87/362 (24.0)	82/327 (25.1)	5/35 (14.3)	17/47 (36.2)	22/82 (26.8)	65/280 (23.2)
Medial	7/87 (8.0)	6/82 (7.3)	1/5 (20.0)	2/17 (11.8)	3/22 (13.6)	4/65 (6.2)
Convexity	30/87 (34.5)	28/82 (34.1)	2/5 (40.0)	2/17 (11.8)	4/22 (18.2)	26/65 (40.0)
Basal	26/87 (29.9)	26/82 (31.7)	0/5 (0)	9/17 (52.9)	9/22 (40.9)	17/65 (26.2)
Sylvian	24/87 (27.6)	22/82 (26.8)	2/5 (40.0)	4/17 (23.5)	6/22 (27.3)	18/65 (27.7)
Total	362 (100)	327 (90.3)	35 (9.7)	47 (13.0)	82 (22.7)	280 (77.3)

All data are presented as number/total (%).

sion or were transgressed microsurgically in at least 1 patient, suggesting that most of the cerebrum was sampled in this cohort.

Patient Outcomes

Good outcomes (mRS score ≤ 2) were observed in 314 of 362 cases (86.7%) and poor outcomes (mRS score > 2) in 25 (6.9%); 23 cases (6.4%) were in patients who were lost to late follow-up. The mean (SD) follow-up duration was 11.5 (22.79) months. Three hundred twenty-seven cases (90.3%) were improved or stable relative to the preoperative neurological condition, and 35 (9.7%) were worse. The cerebral CM subtype was not significantly associated with outcomes (Table 1).

Additional functional decline was observed in 47 of 362 cases (13.0%). The patients in these cases had good relative outcomes with unchanged or improved mRS scores but had other indicators of surgical sequelae. In the combined cohort with poor relative outcomes (35 cases) and additional functional decline (47 cases), 82 of 362 cases (22.7%) had unfavorable outcomes (Table 1, Supplemental Table 1).

Lesion Object Mapping

A machine learning model using SVC identified cerebral CM locations or lesion objects associated with unfavorable outcomes after CM resection. The model identified 33 cortical parcels with collisions detected with a feature importance greater than 0.2 (Table 2, Supplemental Table 2). The model performed with an accuracy of 93% and an AUC of 0.81. Overall, 18 parcels (54%) were located in the right hemisphere. The parcels with the greatest feature importance were left 6r, left SFL, right 52, right Pir, right v23ab, and right PreS, of which 3 were involved with the DMN and 3 with the SMN. Overall, 9 parcels were associated with the DMN, 6 with the VN, 4 with the SN, and 2 each with the CEN and DAN. Seventeen parcels were components of the "big 5" large-scale brain networks (i.e., the CEN, DMN, SN, DAN, and ventral attention network [VAN]), which was an overrepresentation compared with their expected rate in a random sample (chi-square test, p = 0.002). The remaining regions included the ventral diencephalon, left amygdala, hippocampus, parahippocampus, regions in the canonical Broca's and Wernicke's areas (Brodmann area 45 and PHT), and 2 limbic/paralimbic regions.

Trajectory Cylinder Mapping

Of the 60 cases involving subcortical CMs, 12 (20.0%) had poor relative outcomes; this rate was significantly higher than the rate of poor relative outcomes among cases involving cortical CMs (23/302 [7.6%]) (p = 0.003). Therefore, tissue transgressed to reach subcortical lesions in this subgroup was analyzed with a machine learning model using SVC to identify trajectory cylinders associated with unfavorable outcomes after CM resection (Fig. 2). The model identified 20 cortical parcels with collisions detected by a feature importance greater than 0.2 (Table 3, Supplemental Table 3). The model performed with an accuracy of 75% and an AUC of 0.93. This model yielded 13

TABLE 2. Feature importance for the object mapping strategy that leverages an SVC machine learning model to predict which patients experience neurocognitive decline after cerebral CM resection

Functional Region Address (hemisphere)	Feature Importance	Primary Network
6r (lt)	1.010931	SMN
SFL (lt)	1	DMN
52 (rt)	1	SMN
Pir (rt)	1	SMN
v23ab (rt)	1	DMN
PreS (rt)	0.883181	DMN
AAIC (lt)	0.862412	SN
Ventral diencephalon (lt)	0.840592	Subcortical
MI (lt)	0.77123	SN
RSC (lt)	0.733324	DMN
POS2 (lt)	0.723708	DMN
p24 (rt)	0.712424	DMN
V3 (rt)	0.681034	VN
V4 (rt)	0.681034	VN
VMV2 (rt)	0.681034	VN
VMV3 (rt)	0.681034	VN
V6 (lt)	0.658699	VN
V7 (lt)	0.658699	VN
PEF (rt)	0.658558	DAN
pOFC (rt)	0.543881	LN
Pallidum (rt)	0.520327	Subcortical
v23ab (lt)	0.510635	DMN
p32 (rt)	0.5	DMN
Putamen (lt)	0.476663	Subcortical
Hippocampus (lt)	0.459302	Subcortical
Amygdala (lt)	0.424823	Subcortical
Pallidum (lt)	0.424823	Subcortical
a32pr (rt)	0.414532	SN
8Ad (rt)	0.351071	CEN
p32pr (rt)	0.331403	SN
8C (lt)	0.310431	CEN
d32 (rt)	0.271205	DMN
FEF (rt)	0.239835	DAN

AAIC = anterior agranular insular cortex; FEF = frontal eye field; MI = middle insula; PEF = parietal eye field; pOFC = posterior orbitofrontal cortex; POS = parieto-occipital sulcus; RSC = retrosplenial cortex; SFL = superior frontal language; VMV = ventromedial visual areas.
Good performance was achieved (AUC = 0.81, accuracy = 93%).

(65%) parcels of significance within the left hemisphere. The parcels with the greatest feature importance were right 471, left FOP4, left putamen, left 8Ad, and left PEF. Overall, 4 parcels were associated with the DMN, 4 with the SN, and 2 each with the CEN, DAN, VAN, left auditory network, and subcortical parcels. The "big 5" networks were overrepresented compared with their expected rate in a random sample (chi-square test, $p = 0.0007$).

Cerebral Heatmap for Eloquence

The combined results of the lesion object mapping and transcerebral trajectory mapping are represented in a brain model that is a heatmap of cortical eloquence (Fig. 3). Parcels with high feature importance (> 0.2) can be interpreted as hotspots for surgical morbidity, as measured by changes in mRS scores and additional functional decline. These parcels form 7 clusters or areas of eloquence, including the supplementary motor area (SMA, bilateral), anterior cingulate cortex (bilateral), posterior cingulate cortex (bilateral), frontal pole (right), anterior insula (left), mesial temporal lobe (left), and occipital cortex (right).

Discussion

Eloquent Cortex

Eloquence is defined as discourse marked by force and persuasiveness or the art of using such discourse.[22] The cortex that directly controls a distinct and important function like motion or language and whose damage produces a focal neurological deficit is also described as eloquent. Although brain tissue is incapable of forceful discourse per se, the concept of eloquent cortex is deeply ingrained in the neurosurgical lexicon. Korbinian Brodmann used Nissl staining to define 52 cortical regions based on cytoarchitecture, associating eloquent functions like speech with Broca's areas 44 and 45 and Wernicke's areas 39 and 40.[23] Wilder Penfield mapped the cerebral cortex with direct electrical stimulation of the brain and demonstrated that motor and sensory function was organized somatotopically in the cortex to an extent that varied in proportion to its importance and complexity, as captured by the homunculus.[24,25] Spetzler and Martin incorporated eloquence in their AVM grading system, including sensorimotor, visual, and language cortices in their definition of eloquent cortex.[2] These memorable heuristics are so ingrained that neurosurgeons have a heightened awareness of these classically eloquent regions and, consequently, plan transcortical surgery to avoid their transgression. Neurosurgeons who transgress these eloquent regions quickly learn from their mistakes to avoid them the next time. Our experience with superficial cerebral CMs demonstrated strict avoidance of classically eloquent cortex with, for example, only 16 of 362 (4.4%) approaches through the pre- or postcentral gyrus or central sulcus. Instead, routes were selected further anteriorly or posteriorly, or alternatively, patients with classically eloquent CMs were observed.

Despite the imperative not to transgress eloquent cortex, we observed poor outcomes based on mRS scores in 6.9% of cases (25/362) and worsened outcomes in 9.7% (35/362). To uncover the broader effect of CM resection, we included another 13.0% (47/362) of cases in which there was additional functional decline, increasing the overall unfavorable outcome rate to 22.7% (82/362). With this more critical assessment of outcome, a more extensive cerebral heatmap was constructed that better identified areas of microsurgical risk or eloquent noneloquence. It is widely accepted that brainstem CM surgery is performed optimally by maximizing subarachnoid dissection to determine where the CM comes to a pial surface to minimize brain tissue transgression. Similarly, cerebral CM surgery is optimized by

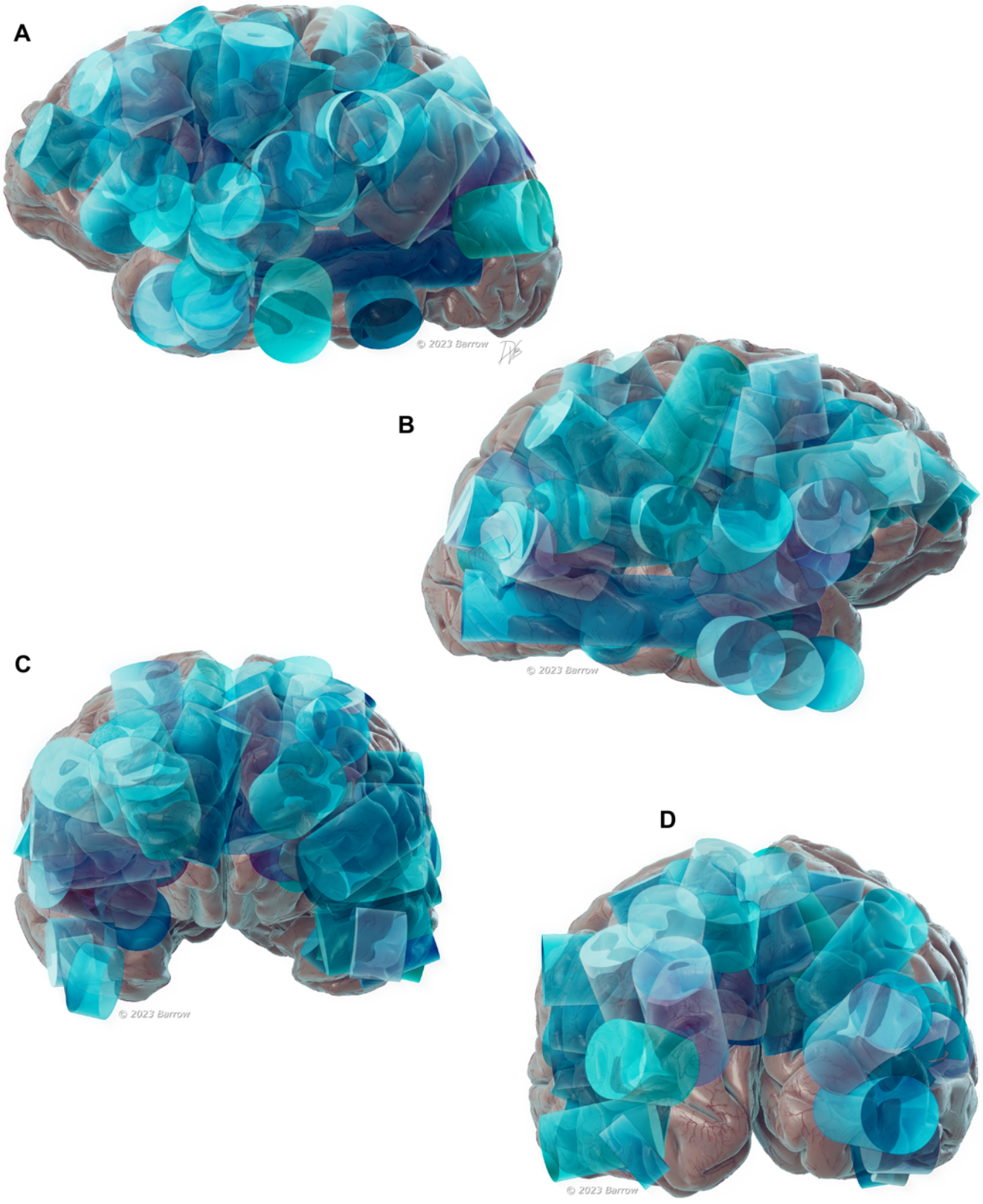

FIG. 2. Left (**A**) and right (**B**) lateral views and anterior (**C**) and posterior (**D**) views showing the deep CM approach trajectories analyzed. Used with permission from Barrow Neurological Institute, Phoenix, Arizona.

TABLE 3. Feature importance for the transcerebral trajectory mapping strategy that leverages an SVC machine learning model to predict which patients experience neurocognitive decline after cerebral CM resection

Functional Region Address (hemisphere)	Feature Importance	Primary Network
471 (rt)	0.56691	VAN
FOP4 (lt)	0.500019	SN
Putamen (lt)	0.457555	Subcortical
8Ad (lt)	0.412382	CEN
PEF (lt)	0.387531	DAN
31a (rt)	0.357876	DMN
PCV (rt)	0.357876	VAN
PI (lt)	0.334497	Auditory
TA2 (lt)	0.334497	Auditory
d23ab (rt)	0.331781	DMN
31pv (rt)	0.329698	DMN
p32pr (lt)	0.301525	SN
47m (lt)	0.288694	LN
AVI (lt)	0.288694	SN
d23ab (lt)	0.23895	DMN
a10p (rt)	0.23573	CEN
Accumbens (rt)	0.221352	Subcortical
55b (lt)	0.217872	Language
i6-8 (lt)	0.217872	DAN
FOP3 (lt)	0.211325	SN

AVI = anterior ventral insula; FOP = frontal operculum; PEF = premotor eye field; PI = posterior insula.
Good performance was achieved (AUC = 0.93, accuracy = 75%).

maximizing transsulcal dissection, shortening the distance to the CM, and minimizing the extent of cortical transgression. We can extrapolate our experience in the brainstem and define cortical SEZs when tissue transgression is unavoidable. We found that cortical SEZs are fewer in number and less safe than expected. Thus, many supposedly noneloquent areas were, in fact, eloquent. The inadequacies of bedside assessments and traditional outcome measures have created a false sense of safety in transcortical surgery. fMRI and connectomics now inform us that large-scale brain networks occupy domains previously considered noneloquent. Dissection through these regions may not be as safe as expected, and flawed or outdated notions of eloquence may explain the functional and cognitive consequences observed in our patients.

Large-Scale Brain Networks

Large-scale brain networks (Figs. 4 and 5), or intrinsic brain networks, are collections of regions throughout the brain connected structurally and functionally as demonstrated by fMRI blood oxygen level–dependent signaling or other modalities like PET, magnetoencephalography, or EEG.[9,11,21] These widespread parcellations or nodes have interconnecting white matter tracts and exhibit synchronized activity during complex tasks. Large-scale brain networks include 7 major networks (DMN, CEN or control, SN, DAN, SMN, VN, and LN) as well as other networks (VAN, language, accessory language, auditory, multiple demand, and medial temporal networks).[8,9,11,21] The areas of unexpected surgical morbidity in our cerebral heatmap for eloquence may appear random (Tables 2 and 3) but are understandable from the perspective of large-scale network disruption. Parcellations with high feature importance are parts of the central core of key networks or connect that network to others (i.e., "hubness").

The DMN is one of the largest networks based on cortical territory and is active when the individual is awake, at rest, and engaged in the internal activity of the mind, which includes daydreaming, passive sensory processing, envisioning, and memory retrieval.[7,26] This network is one of the most active, working when the individual is not engaged in external tasks (task-negative system) or focused on external visual signals. The DMN is centered in the medial frontoparietal cortex, but its parcellations extend throughout all lobes and surfaces.

The CEN initiates and modulates cognitive control and is associated with intelligence, thought, decision-making, and executive function.[27–30] This network works when the individual is engaged in external tasks (task-positive system) and is inversely associated with the activity of the DMN. External thinking during active tasks, planning, and problem-solving requires working memory and attention, thereby engaging other key networks simultaneously. The CEN is located in the bilateral frontal and parietal convexities.

The SN monitors the significance of external and internal inputs, directing engagement by identifying important biological activity and cognitive events.[29,31–33] The SN acts as a switch that transitions between the resting state of the DMN and the active state of the CEN, activating and deactivating these 2 key networks. The SN monitors the external world to decide how other networks react to new information and stimuli. Pain sensation, emotions, and motivational states are surveyed, and the activity of other networks is modulated accordingly to establish the brain's reaction to these inputs. The SN is centered in the anterior cingulate cortex and anterior insula.

The DAN actively orients and holds attention during goal-directed tasks and executive functions.[27,34,35] Top-down processing is the intentional control of behavior or performance that enables the individual to focus on an activity and ignore environmental or biological stimuli or noise. In contrast, bottom-up processing is the response to environmental or biological stimuli that switches attention to important signals and often interrupts higher cognitive activity. The VAN calls attention to these other sensory stimuli and noises. The VAN is often inhibited during top-down focused attention to prevent distraction by irrelevant stimuli. The DAN is located bilaterally in the intraparietal sulci and frontal eye fields, and the VAN is in the right-sided temporoparietal junction and ventral frontal cortex.

Hotspots of Cerebral Eloquence

The context of large-scale brain networks can explain the surgical morbidity observed in our experience with superficial cerebral CMs, with the 7 hotspots in our heatmap

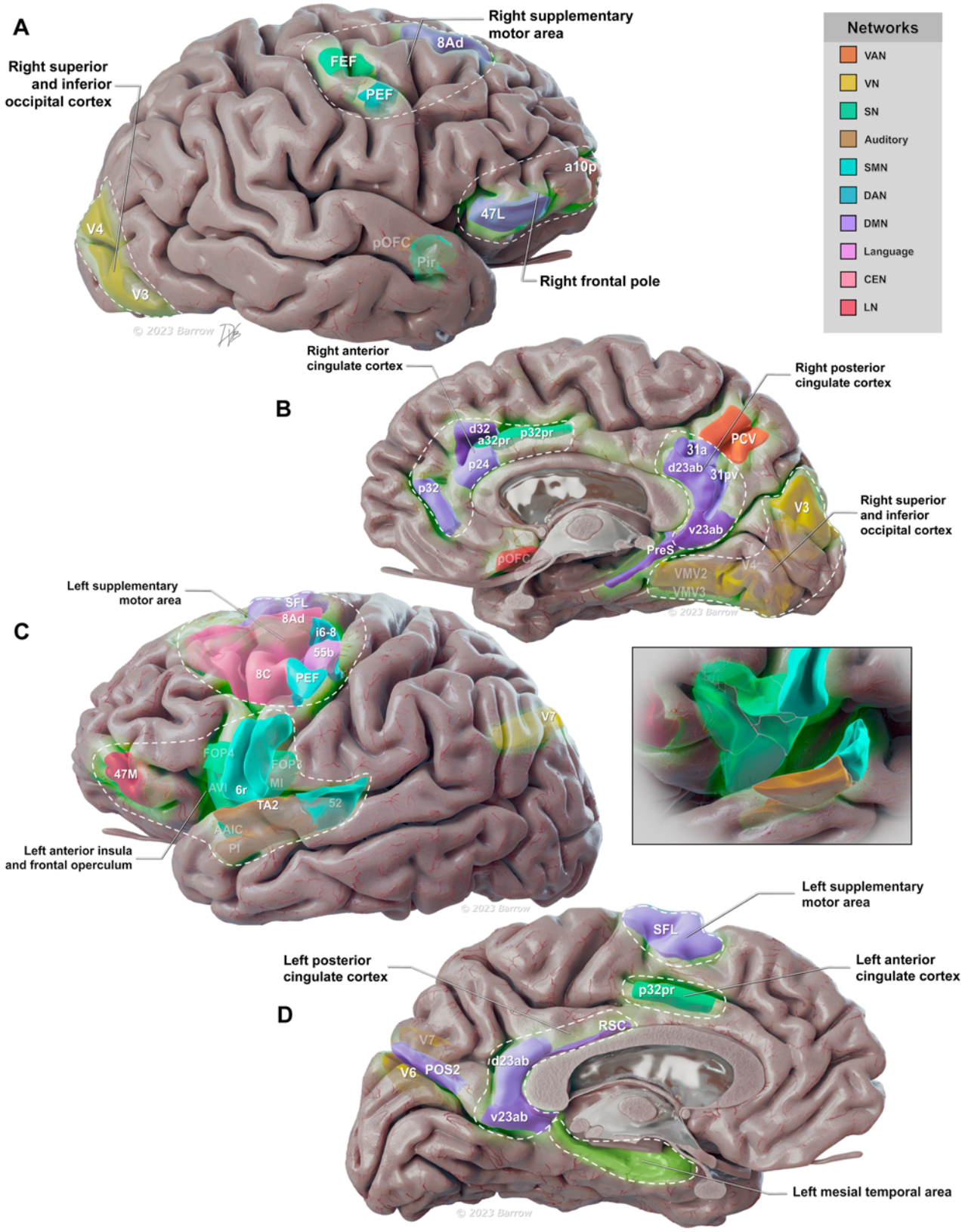

FIG. 3. Heatmap of cerebral eloquence with 7 key hotspots: SMA (bilateral), anterior cingulate cortex (bilateral), posterior cingulate cortex (bilateral), anterior insula (left), frontal pole (right), mesial temporal lobe (left), and occipital cortex (right). Images show the anatomical locations of the 7 hotspots of functional risk as dashed shapes encircling the clusters of parcels in the model. *White labels* represent parcel addresses. Right lateral (**A**), left medial (**B**), left lateral (**C**), and right medial (**D**) views are shown. Note that the label color reflects the network affiliation of the relevant regions. The **inset** depicts parcels in the left anterior insula, which is one of the 7 key hotspots. Used with permission from Barrow Neurological Institute, Phoenix, Arizona.

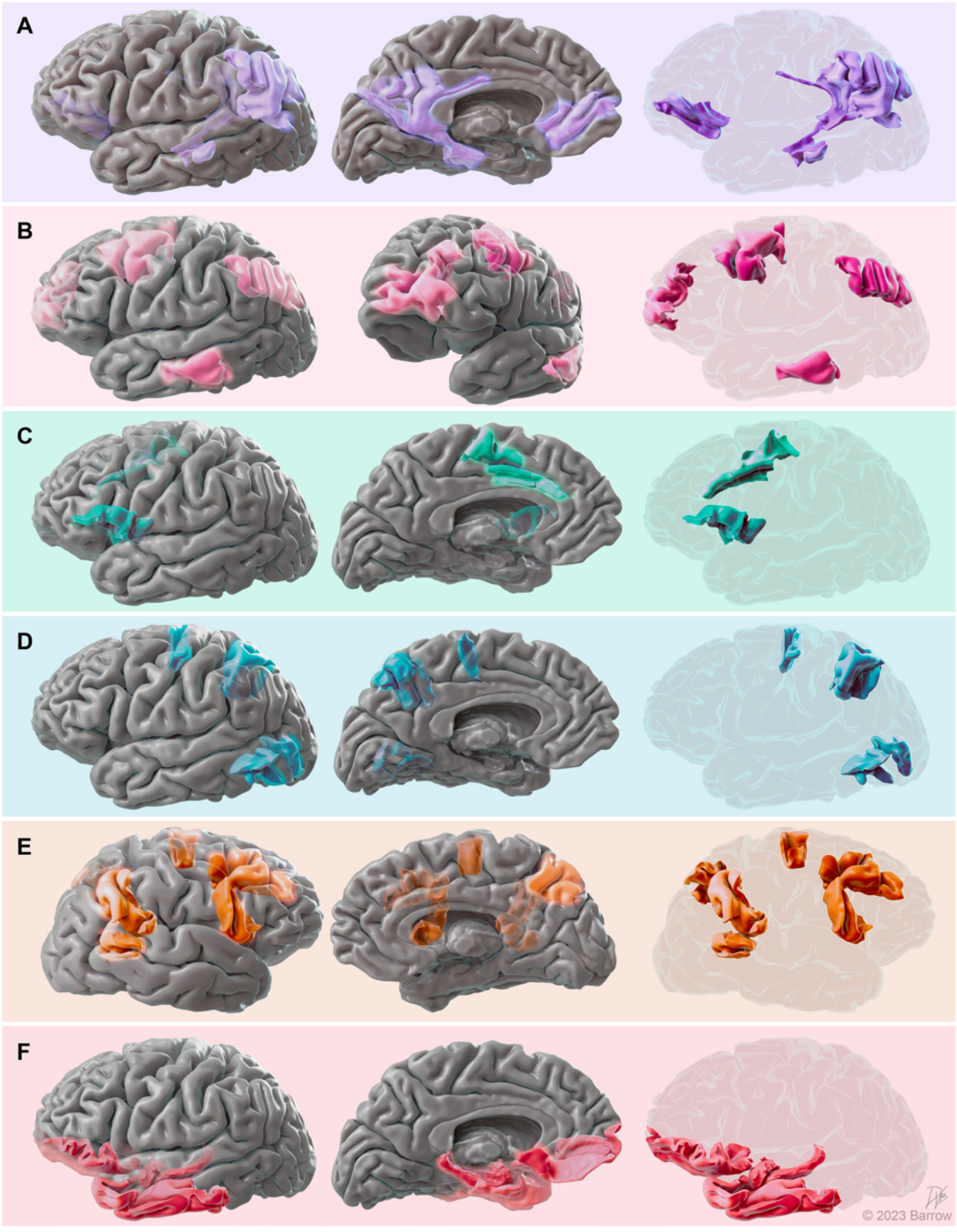

FIG. 4. Large-scale brain networks include 7 major networks (DMN, CEN, SN, DAN, SMN, VN, and LN) as well as other networks (VAN, language, accessory language, auditory, multiple demands, and medial temporal networks). Six key brain networks are shown: DMN (**A**), CEN (**B**), SN (**C**), DAN (**D**), VAN (**E**), and LN (**F**). The *left column* shows the left (A, B, C, D, and F) or right (E) cerebral hemisphere from a lateral perspective, the *middle column* shows the same cerebral hemisphere from a medial perspective, and the *right column* shows the network in isolation. Used with permission from Barrow Neurological Institute, Phoenix, Arizona.

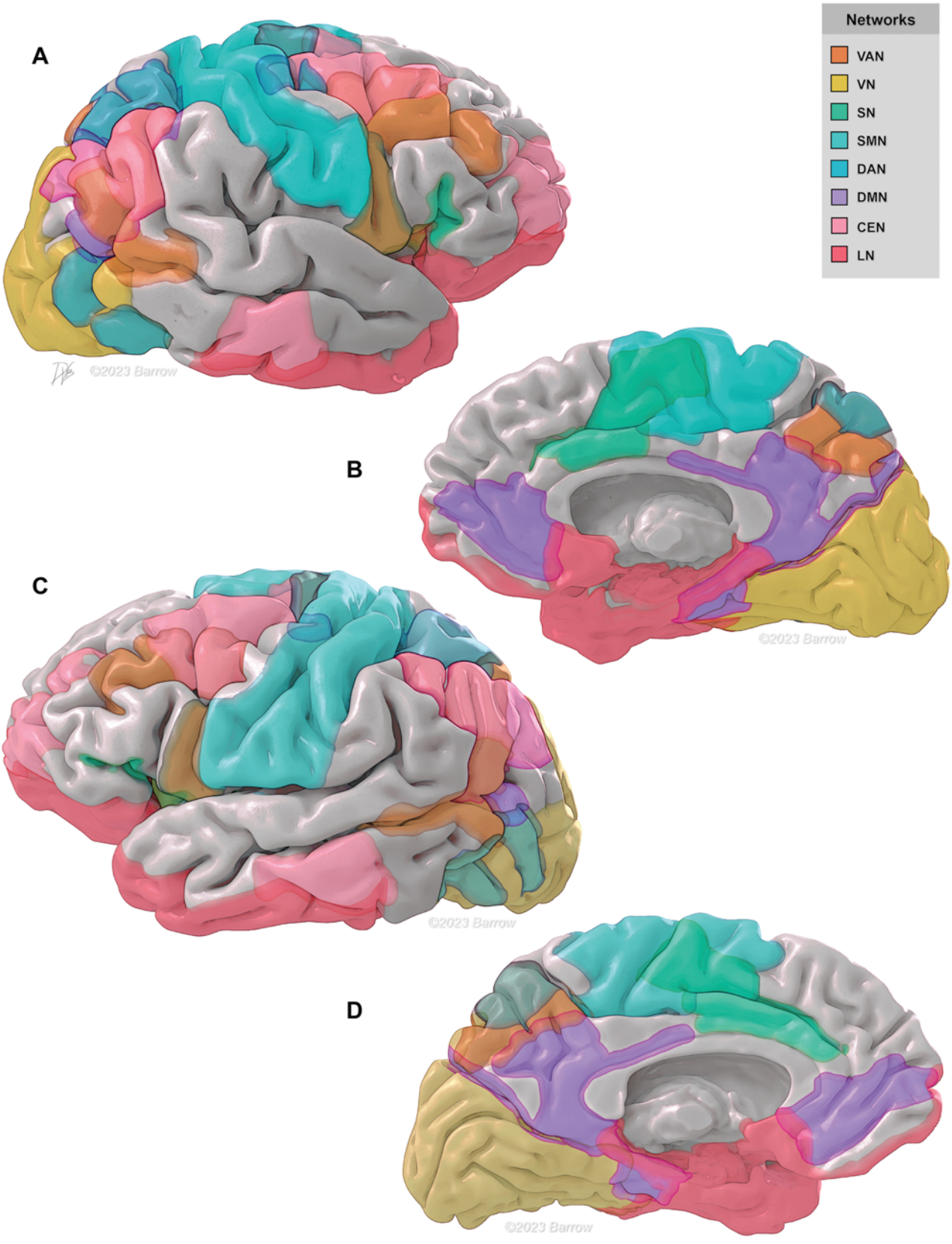

FIG. 5. Large-scale brain networks are demonstrated in a synoptic graphic, including the VAN, VN, SN, SMN, DAN, DMN, CEN, and LN. The graphic shows the right cerebral hemisphere from lateral (**A**) and medial (**B**) perspectives and the left cerebral hemisphere from lateral (**C**) and medial (**D**) perspectives. Used with permission from Barrow Neurological Institute, Phoenix, Arizona.

corresponding to transgression to key regions of major networks (Fig. 6). The SMA, the first of these hotspots, occupies the posterior third of the superior frontal gyrus and helps plan and initiate movement. With the SMN being one of the most important networks (3 of the top 5 parcellations with feature importance on lesion mapping), few approaches were taken through pre- or postcentral gyri or the central sulcus (16/362, 4.4%). However, alternative approaches were taken through the adjacent SMA (precentral sulcus, superior frontal sulcus, superior frontal gyrus, inferior frontal sulcus, etc.) to protect the SMN from transgression. The SMA was exploited as an anterior route to motor CMs; it emerged as an eloquent hotspot. The SMA syndrome, or transient hemiplegia and mutism after cortical transgression or resection in the medial or convexity portions of the superior frontal gyrus, shows the degree of interconnectedness or hubness of networks in this region. Six parcellations with feature importance in the left SMA belong to 5 networks and their white matter tracts, including the frontal aslant tract, link SMA to premotor areas, Broca's area, and the SN for motor and speech initiation.[36–38]

The anterior and posterior cingulate gyri also emerged as eloquent hotspots, which can explain their importance to the DMN and SN. Nine parcellations in the DMN and 4 in SN had feature importance in lesion mapping, and 4 parcellations in the DMN and SN had feature importance in trajectory mapping. The anterior and posterior cingulate gyri are noneloquent areas straddling the leg sensorimotor cortex. Consequently, interhemispheric approaches to medial frontal and parietal CMs often transgressed these areas. Gravity-assisted dissection of the interhemispheric fissure, with the midline of the head positioned horizontally for gravity retraction of the dependent hemisphere, made this route a frequent choice for medial CM subtypes. An underappreciation of the DMN and SN could have contributed to their surgical disruption. Gravity-assisted interhemispheric approaches should remain first-line exposures for medial CMs, perhaps with more transsulcal dissections to reach the target and greater respect for these 2 core networks.

The left anterior insula emerged as an eloquent hotspot partly because of its proximity to 6r, the parcellation with the highest feature importance on lesion mapping and part of the SMN involved in speech.[17,39] In addition, 2 parcellations in the auditory network had high feature importance on trajectory mapping, indicating the significance of the auditory cortex on the temporal side of the sylvian fissure. Anterior insular CMs are not included with superficial cerebral CMs but are deep cerebral CMs because they abut the caudate nucleus and putamen. However, sylvian CMs are included with superficial cerebral CMs and require transsylvian dissection for their resection. Anterior insular eloquence requires meticulous dissection technique when transsylvian routes are taken on the dominant side, especially when the M2 insular segments of the middle cerebral artery are intimately involved in the dissection.

The right frontal pole was the hotspot with the least expected eloquence. This nondominant frontal pole is often considered noneloquent because its removal does not cause hemiparesis, aphasia, or coma. However, it participates in behavior, socialization, and impulse control. Frontal pole parcels with feature importance belonged to the CEN and VAN. Overall, the CEN had just 2 parcellations with feature importance in lesion mapping and 2 in trajectory mapping. CEN transgressions might have been detected in high-functioning patients due to our inclusion of additional functional decline. In contrast to the right frontal pole, the left mesial temporal and right occipital hotspots are less surprising for their eloquence, given their recognized involvement in memory function and visual perception, respectively. It is worth noting that the hippocampus is not included in the definition of eloquence in the Spetzler-Martin AVM grading system. The side of the mesial temporal hotspot suggests that functional decline may be due to effects on verbal memory. The right-sided occipital hotspot is thought to be due to its role in visuospatial processing.

Study Limitations

We defined cortical hotspots as unsafe entry zones, in contrast to our previous work that defined cortical SEZs, to guide the transgression of cortical tissue, avoid eloquent areas, and reduce unfavorable outcomes. These hotspots further our conceptualization of eloquence when added to the motor and sensory strips, visual cortex, Broca's and Wernicke's areas, and the auditory areas on the cortical map. It would be erroneous to conclude that all areas outside the 7 hotspots are cortical SEZs. The study findings suggest that increasing the extent of subarachnoid and transgyral dissection and performing intracapsular rather than extracapsular resections might improve outcomes. However, our analysis is retrospective, and the impact of these technical modifications is speculative. The benefits of minimalistic, tissue-sparing techniques are clear from the positive results of the recently released ENRICH (Early Minimally Invasive Removal of Intracerebral Hemorrhage) trial demonstrating improved functional outcomes in the surgical group relative to medical management, especially in the context of previously negative results from STICH (Surgical Trial in Intracerebral Haemorrhage).[40,41]

We included large-scale brain networks in our interpretation of this experience because human connectomics helps us understand our outcomes and improve our microsurgical technique. This sophisticated analysis depended on the Quicktome machine learning algorithm for parcel designation, tissue transgression analysis, and calculation of feature importance. Although these methods and metrics are unfamiliar to most neurosurgeons, they are validated by the literature in related disciplines like computational neurosciences.[8] Our methodology emphasized the size of parcel and network disruption (collisions) rather than the location of that disruption within a network (centrality) or the interconnections with other networks (hubness), which may be important factors. Our database included a large cohort of highly selected surgical patients with robust radiographic imaging. Cognitive outcomes were of particular interest, but detailed neuropsychological tests were not available. Conventional neurological outcomes, as measured by mRS scores, were augmented by the additional functional decline factor as a real-world surrogate for cognitive outcomes, but this crude metric

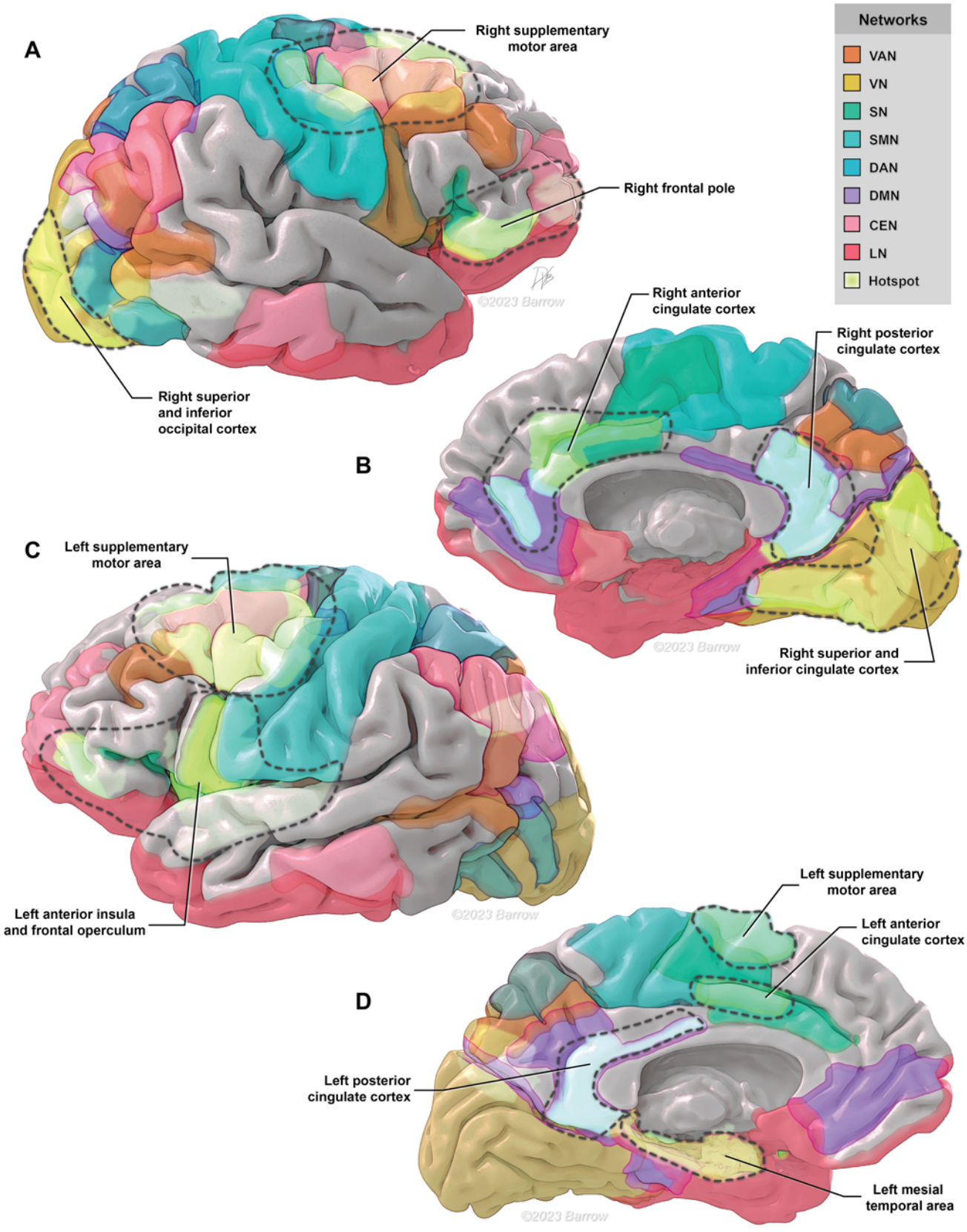

FIG. 6. Large-scale brain networks are shown with an overlay of the 7 hotspots (*black dashed outlines*) identified in the study. Large-scale brain networks include the VAN, VN, SN, SMN, DAN, DMN, CEN, and LN. The graphic shows the right cerebral hemisphere from lateral (**A**) and medial (**B**) perspectives and the left cerebral hemisphere from lateral (**C**) and medial (**D**) perspectives. Used with permission from Barrow Neurological Institute, Phoenix, Arizona.

may not correlate with neuropsychological metrics. Complete pre- and postoperative neuropsychological and cognitive testing is needed to assess our surgical outcomes. Finally, we relied on a single brain template for lesion and trajectory mapping. fMRI quality was not uniform across the cohort and needed to be sufficiently high for comprehensive connectomic analysis. Warping individualized lesion volumes and trajectories onto a single brain model resulted in some loss of accuracy because individualized brain anatomy is lost.

Conclusions

The microsurgical management of superficial cerebral CMs has relied on transgyral and transsulcal resections that circumvent areas of traditional eloquence and navigate areas presumed to be noneloquent. This study demonstrates that areas of the brain long considered by neurosurgeons to be noneloquent are actually eloquent. A machine learning analysis of lesion and trajectory mapping in this large cohort identified 7 hotspots of eloquence within multiple large-scale networks: 1) SMA (bilateral), 2) anterior cingulate cortex (bilateral), 3) posterior cingulate cortex (bilateral), 4) anterior insula (left), 5) frontal pole (right), 6) mesial temporal lobe (left), and 7) occipital cortex (right). These eloquent areas previously considered to be noneloquent redefine our neurosurgical concept of eloquence and suggest a need for more refined transcortical dissection techniques that maximize transsulcal dissection, intracapsular resection, and tissue preservation. Human connectomics, awareness of large-scale brain networks, and prioritization of cognitive outcomes require that we update our concept of cortical eloquence and incorporate this information into our surgical strategies and navigational tools.

Acknowledgments

We thank the staff of Neuroscience Publications at Barrow Neurological Institute for assistance with manuscript preparation. We also thank Hugh Taylor, Negar Mansouri, Michael Sughrue, MD, and Peter Rudder from Omniscient Neurotechnology, Sydney, Australia, for their assistance with the machine learning analysis.

References

1. James W. The energies of men. *Science*. 1907;25(635):321-332.
2. Spetzler RF, Martin NA. A proposed grading system for arteriovenous malformations. *J Neurosurg*. 1986;65(4):476-483.
3. Van Essen DC, Ugurbil K, Auerbach E, et al. The Human Connectome Project: a data acquisition perspective. *Neuroimage*. 2012;62(4):2222-2231.
4. Moeller S, Yacoub E, Olman CA, et al. Multiband multislice GE-EPI at 7 tesla, with 16-fold acceleration using partial parallel imaging with application to high spatial and temporal whole-brain fMRI. *Magn Reson Med*. 2010;63(5):1144-1153.
5. Sotiropoulos SN, Moeller S, Jbabdi S, et al. Effects of image reconstruction on fiber orientation mapping from multichannel diffusion MRI: reducing the noise floor using SENSE. *Magn Reson Med*. 2013;70(6):1682-1689.
6. Foster BL, Parvizi J. Resting oscillations and cross-frequency coupling in the human posteromedial cortex. *Neuroimage*. 2012;60(1):384-391.
7. Buckner RL, Andrews-Hanna JR, Schacter DL. The brain's default network: anatomy, function, and relevance to disease. *Ann N Y Acad Sci*. 2008;1124:1-38.
8. Baker CM, Burks JD, Briggs RG, et al. A connectomic atlas of the human cerebrum-chapter 1: introduction, methods, and significance. *Oper Neurosurg (Hagerstown)*. 2018;15(suppl 1):S1-S9.
9. Yeo BT, Krienen FM, Sepulcre J, et al. The organization of the human cerebral cortex estimated by intrinsic functional connectivity. *J Neurophysiol*. 2011;106(3):1125-1165.
10. Eickhoff SB, Yeo BTT, Genon S. Imaging-based parcellations of the human brain. *Nat Rev Neurosci*. 2018;19(11):672-686.
11. Doucet GE, Lee WH, Frangou S. Evaluation of the spatial variability in the major resting-state networks across human brain functional atlases. *Hum Brain Mapp*. 2019;40(15):4577-4587.
12. Morez J, Sijbers J, Vanhevel F, Jeurissen B. Constrained spherical deconvolution of nonspherically sampled diffusion MRI data. *Hum Brain Mapp*. 2021;42(2):521-538.
13. Glasser MF, Coalson TS, Robinson EC, et al. A multimodal parcellation of human cerebral cortex. *Nature*. 2016;536(7615):171-178.
14. Ren H, Zhu J, Su X, et al. Application of structural and functional connectome mismatch for classification and individualized therapy in Alzheimer disease. *Front Public Health*. 2020;8:584430.
15. Briggs RG, Conner AK, Baker CM, et al. A connectomic atlas of the human cerebrum-chapter 18: the connectional anatomy of human brain networks. *Oper Neurosurg (Hagerstown)*. 2018;15(suppl 1):S470-S480.
16. Allan PG, Briggs RG, Conner AK, et al. Parcellation-based tractographic modeling of the dorsal attention network. *Brain Behav*. 2019;9(10):e01365.
17. Allan PG, Briggs RG, Conner AK, et al. Parcellation-based tractographic modeling of the ventral attention network. *J Neurol Sci*. 2020;408:116548.
18. Kuiper JJ, Lin YH, Young IM, et al. A parcellation-based model of the auditory network. *Hear Res*. 2020;396:108078.
19. Sheets JR, Briggs RG, Bai MY, et al. Parcellation-based modeling of the dorsal premotor area. *J Neurol Sci*. 2020;415:116907.
20. Sheets JR, Briggs RG, Dadario NB, et al. A cortical parcellation based analysis of ventral premotor area connectivity. *Neurol Res*. 2021;43(7):595-607.
21. Briggs RG, Young IM, Dadario NB, et al. Parcellation-based tractographic modeling of the salience network through meta-analysis. *Brain Behav*. 2022;12(7):e2646.
22. eloquence. Merriam-Webster. Accessed December 26, 2023. https://www.merriam-webster.com/dictionary/eloquence
23. Brodmann K. *Vergleichende Lokalisationslehre der Grosshirnrinde in ihren Prinzipien dargestellt auf Grund des Zellenbaues*. Johann Ambrosius Barth Verlag; 1909.
24. Penfield W, Boldrey E. Somatic motor and sensory representation in the cerebral cortex of man as studied by electrical stimulation. *Brain*. 1937;60(4):389-443.
25. Rasmussen T, Penfield W. Further studies of the sensory and motor cerebral cortex of man. *Fed Proc*. 1947;6(2):452-460.
26. Tanglay O, Young IM, Dadario NB, et al. Anatomy and white-matter connections of the precuneus. *Brain Imaging Behav*. 2022;16(2):574-586.
27. Boord P, Madhyastha TM, Askren MK, Grabowski TJ. Executive attention networks show altered relationship with default mode network in PD. *Neuroimage Clin*. 2016;13:1-8.
28. Chen AC, Oathes DJ, Chang C, et al. Causal interactions between fronto-parietal central executive and default-mode networks in humans. *Proc Natl Acad Sci U S A*. 2013;110(49):19944-19949.
29. Ellard KK, Zimmerman JP, Kaur N, et al. Functional connec-

tivity between anterior insula and key nodes of frontoparietal executive control and salience networks distinguish bipolar depression from unipolar depression and healthy control subjects. *Biol Psychiatry Cogn Neurosci Neuroimaging*. 2018; 3(5):473-484.
30. Firbank M, Kobeleva X, Cherry G, et al. Neural correlates of attention-executive dysfunction in lewy body dementia and Alzheimer's disease. *Hum Brain Mapp*. 2016;37(3):1254-1270.
31. Balaev V, Orlov I, Petrushevsky A, Martynova O. Functional connectivity between salience, default mode and frontoparietal networks in post-stroke depression. *J Affect Disord*. 2018; 227:554-562.
32. Bonnelle V, Ham TE, Leech R, et al. Salience network integrity predicts default mode network function after traumatic brain injury. *Proc Natl Acad Sci U S A*. 2012;109(12):4690-4695.
33. Chang YT, Lu CH, Wu MK, et al. Salience network and depressive severities in Parkinson's disease with mild cognitive impairment: a structural covariance network analysis. *Front Aging Neurosci*. 2018;9:417.
34. Catalino MP, Yao S, Green DL, Laws ER, Golby AJ, Tie Y. Mapping cognitive and emotional networks in neurosurgical patients using resting-state functional magnetic resonance imaging. *Neurosurg Focus*. 2020;48(2):E9.
35. Corbetta M, Shulman GL. Spatial neglect and attention networks. *Annu Rev Neurosci*. 2011;34:569-599.
36. Dadario NB, Brahimaj B, Yeung J, Sughrue ME. Reducing the cognitive footprint of brain tumor surgery. *Front Neurol*. 2021;12:711646.
37. Dick AS, Garic D, Graziano P, Tremblay P. The frontal aslant tract (FAT) and its role in speech, language and executive function. *Cortex*. 2019;111:148-163.
38. La Corte E, Eldahaby D, Greco E, et al. The frontal aslant tract: a systematic review for neurosurgical applications. *Front Neurol*. 2021;12:641586.
39. Ventral attention network (VAN). Quicktome Connectome Guide 2021. Omniscient Neurotechnology. Accessed December 26, 2023. https://quicktome.o8t.com/guide/network/ventral-attention-network
40. ENRICH Trial findings debuts at the 2023 American Association of Neurological Surgeons Annual Scientific Meeting. AANS. April 17, 2023. Accessed December 26, 2023. https://www.newswise.com/articles/enrich-trial-findings-debuts-at-the-2023-american-association-of-neurological-surgeons-annual-scientific-meeting
41. Mendelow AD, Gregson BA, Rowan EN, Murray GD, Gholkar A, Mitchell PM. Early surgery versus initial conservative treatment in patients with spontaneous supratentorial lobar intracerebral haematomas (STICH II): a randomised trial. *Lancet*. 2013;382(9890):397-408.

Disclosures

The authors report no conflict of interest concerning the materials or methods used in this study or the findings specified in this paper.

Author Contributions

Conception and design: Lawton, Hendricks. Acquisition of data: Lawton, Hendricks, Scherschinski, Jubran, Dadario, Karahalios, Benner. Analysis and interpretation of data: Lawton, Hendricks, Jubran, Dadario, Benner. Drafting the article: Lawton, Hendricks, Dadario. Critically revising the article: Lawton, Hendricks, Benner. Reviewed submitted version of manuscript: Lawton, Hendricks, Dadario, Benner. Approved the final version of the manuscript on behalf of all authors: Lawton. Statistical analysis: Hendricks. Administrative/technical/material support: Lawton, Hendricks. Study supervision: Lawton, Hendricks. Medical illustrations: VanBrabant.

Supplemental Information

Online-Only Content

Supplemental material is available with the online version of the article.

Supplemental Tables 1–3. https://thejns.org/doi/suppl/10.3171/2023.12.JNS232588.

Correspondence

Michael T. Lawton: c/o Neuroscience Publications, Barrow Neurological Institute, St. Joseph's Hospital and Medical Center, Phoenix, AZ. neuropub@barrowneuro.org.